

# Comparison of two methods for calculating nucleation rates

G. Münster<sup>a</sup>, A. Strumia<sup>b</sup> and N. Tetradis<sup>c</sup>

(a) *Institut für Theoretische Physik I, Universität Münster  
Wilhelm-Klemm-Str. 9, D-48149 Münster, Germany*

(b) *Dipartimento di Fisica, Università di Pisa and INFN, I-56127 Pisa, Italia*

(c) *Scuola Normale Superiore, Piazza dei Cavalieri 7, I-56126 Pisa, Italy and  
Department of Physics, University of Athens, GR-15771 Athens, Greece*

## Abstract

First-order phase transitions that proceed via nucleation of bubbles are described by the homogeneous nucleation theory of Langer. The nucleation rate is one of the most interesting parameters of these transitions. In previous works we have computed nucleation rates with two different methods: ( $\mathcal{A}$ ) employing coarse-grained potentials; ( $\mathcal{B}$ ) by means of a saddle-point approximation, using dimensionally regularized field theory. In this article we compare the results of the two approaches in order to test their reliability and to determine the regions of applicability. We find a very good agreement.

## 1 Introduction

The calculation of bubble-nucleation rates during first-order phase transitions is a difficult problem with a long history. It has applications to a variety of physical situations, ranging from the metastability of statistical systems, such as supercooled liquids or vapours [1], to cosmological phase transitions, such as the electroweak or the deconfinement phase transition in QCD [2]. (For reviews with an extensive list of references, see refs. [1, 2, 3, 4, 5].) Our present understanding of the phenomenon of nucleation is based largely on the work of Langer [6]. In the absence of impurities in the system, Langer's approach is characterized as homogeneous nucleation theory. The basic assumption is that the system in the metastable phase is in a state of quasi-equilibrium. The nucleation rate is proportional to the imaginary part of the analytic continuation of the equilibrium free energy into the metastable phase. The rate can be calculated by considering fluctuations of the system around particular configurations characterized as critical bubbles or droplets. They are saddle points of the free energy and drive the nucleation process. Extensive studies have been carried out within this framework in the last decades. (See the reviews [1, 2, 3, 4, 5], and ref. [7] for work in the context of field theory.) Also alternative approaches have been pursued, that do not rely on the explicit introduction of droplets [8].

We employ here the application of Langer's approach to field theory [9, 10]. The basic quantity of interest is the nucleation rate  $I$ , which gives the probability per unit time and volume to nucleate a certain region of the stable phase (the true vacuum) within the metastable phase (the false vacuum). The calculation of  $I$  relies on an expansion around a dominant semiclassical saddle-point that is identified with the critical bubble or droplet. This is a static configuration (usually assumed to be spherically symmetric) within the metastable phase whose interior consists of the stable phase. It has a certain radius that can be determined from the parameters of the

underlying theory. Bubbles slightly larger than the critical one expand rapidly, thus converting the metastable phase into the stable one.

The bubble-nucleation rate is exponentially suppressed by the action (the free energy rescaled by the temperature) of the critical bubble. Possible deformations of the critical bubble generate a static pre-exponential factor. The leading contribution to it has the form of a ratio of fluctuation determinants and corresponds to the first-order correction to the semiclassical result. Apart from the static prefactor, the nucleation rate includes a dynamical prefactor that takes into account the expansion of bubbles after their nucleation. We concentrate only on the static aspects of the problem and neglect the dynamical prefactor.

We consider a three-dimensional statistical system with one space-dependent degree of freedom described by a real scalar field  $\phi(x)$ . For example,  $\phi(x)$  may correspond to the density for the gas/liquid transition, or to a difference in concentrations for chemical phase transitions, or to the magnetization for the ferromagnetic transition. Our discussion also applies to a (3+1)-dimensional quantum field theory in quasi-thermal equilibrium for energy scales below the temperature. Then an effective three-dimensional description applies [11]. In a different context our results can also be applied to the problem of quantum tunnelling in a (2+1)-dimensional field theory at zero temperature.

The bubble-nucleation rate is given by [6, 9]

$$I = A \exp(-S_b) = \frac{E_0}{2\pi} \left( \frac{S_b}{2\pi} \right)^{3/2} \left| \frac{\det'[\delta^2 S/\delta\phi^2]_{\phi=\phi_b}}{\det[\delta^2 S/\delta\phi^2]_{\phi=0}} \right|^{-1/2} \exp(-S_b). \quad (1)$$

Here  $S$  is the action of the system for a given configuration of the field  $\phi$ . For statistical systems the parameters appearing in  $S$  can be related to those in the Hamiltonian (see [12] for an example). The action of the critical bubble is  $S_b = S(\phi_b(r)) - S(0)$ , where  $\phi_b(r)$  is the spherically-symmetric bubble configuration and  $\phi = 0$  corresponds to the false vacuum. The fluctuation determinants are evaluated either at  $\phi = 0$  or around  $\phi = \phi_b(r)$ . The prime in the fluctuation determinant around the bubble denotes that the three zero eigenvalues of the operator  $[\delta^2 S/\delta\phi^2]_{\phi=\phi_b}$  have been removed. Their contribution generates the factor  $(S_b/2\pi)^{3/2}$  and the volume factor that is absorbed in the definition of  $I$  (nucleation rate per unit volume). The quantity  $E_0$  is the square root of the absolute value of the unique negative eigenvalue.

The calculation of the pre-exponential factor  $A$  is a technically difficult problem. In this letter we compare the results of two different methods for its evaluation in order to confirm their reliability. The first method, described in refs. [13, 12] and denoted by  $\mathcal{A}$  in the following, is based on the notion of coarse graining and employs the Wilson approach to the renormalization group [14] in the formulation of the effective average action [15]. It can be applied to a multitude of systems described by a variety of actions. In the second method, described in ref. [16] and denoted by  $\mathcal{B}$ , the nucleation rate is calculated analytically near the so-called thin-wall limit. Starting from a bare action with a quartic potential, the bubble solution, its action, and the fluctuation determinants are obtained as power-series in an asymmetry parameter, which is small near the thin-wall limit. Renormalization is performed in the context of dimensional regularization near 3 dimensions.

## 2 Relation between coarse graining and dimensional regularization

In ref. [16] nucleation rates were calculated for a model described by the bare action<sup>1</sup>

$$S_0 = \int d^3x [K_0 - V_0] = \int d^3x \left[ \frac{(\partial\phi)^2}{2} - \frac{m^2}{2}\phi^2 - \frac{\gamma}{6}\phi^3 - \frac{g}{8}\phi^4 \right]. \quad (2)$$

This potential has the typical form relevant for first-order phase transitions in (3+1)-dimensional field theories at high temperature. Through a shift  $\phi \rightarrow \phi + c$  the cubic term can be eliminated in favour of a term linear in  $\phi$ . As a result the same potential can describe statistical systems of the Ising universality class in the presence of an external magnetic field. The calculation was performed in the limit that the asymmetry parameter is small and the two minima of the potential have nearly equal depth. The critical bubbles are not far from the thin-wall limit: The width of the surface is much smaller than the radius.

<sup>1</sup>This model has a special feature: when the two minima are taken to be exactly degenerate a  $Z_2$  symmetry guarantees that they are equivalent. Therefore the thin-wall limit of more generic models without this particular feature can be qualitatively different.

We would like to verify that the predictions of method  $\mathcal{A}$  are in agreement with those of method  $\mathcal{B}$ . In order to make the comparison we must understand how to find a coarse-grained action equivalent to a bare or renormalized one in the framework of dimensional regularization. This can be done by requiring that the two versions of the same theory describe the same physics. In the one-loop approximation we can require that the same effective potential is obtained in both cases. With dimensional regularization, the one-loop effective potential is

$$V_1 = V_0 - \frac{1}{12\pi}(V_0'')^{3/2}. \quad (3)$$

Since poles in  $\epsilon = 3 - d$  only appear at the two-loop level, in the one-loop approximation the minimally renormalized parameters are equal to the bare ones. If desired, they can be related to physical observables via finite renormalization corrections [17, 16].

On the other hand, the coarse graining employed in method  $\mathcal{A}$  can be implemented by introducing an effective infrared cutoff that acts as a mass term  $\sim k^2$  [13, 12]. The coarse-grained potential  $V_k$  becomes the effective potential for  $k = 0$ . Only fluctuations with characteristic momenta  $0 \lesssim q^2 \lesssim k^2$  contribute to the expression that relates  $V_{k=0}$  and  $V_k$ :

$$V_1 = V_{k=0} = V_k - \frac{1}{12\pi}[V_k''^{3/2} - (k^2 + V_k'')^{3/2}]. \quad (4)$$

The one-loop effective potential  $V_1$  is complex for values of  $\phi$  such that  $V_k'' < 0$ . This pathology of the one-loop approximation could be avoided solving numerically the exact renormalization-group equation for  $V_k$ . However, the same problem appears at one loop in the dimensionally regularized version of the theory, eq. (3), and cancels out when matching the two versions of the theory. Therefore, at one-loop order, the coarse-grained potential  $V_k$  corresponding to a given bare potential  $V_0$  employed in dimensional regularization is

$$V_k = V_0 - \frac{1}{12\pi}(k^2 + V_0'')^{3/2}. \quad (5)$$

In the context of method  $\mathcal{A}$  the calculation of nucleation rates is performed at values of  $k$  sufficiently large that the one-loop approximation for  $V_k$ , eq. (5), is real for all  $\phi$ .

In method  $\mathcal{A}$  we neglect the corrections to terms with derivatives of the field in the coarse-grained action, keeping only the corrections to the effective potential. We have verified that including also the field-dependent one-loop correction to the kinetic term has a negligible influence on the following results.

### 3 Comparison of the two methods

It is convenient to use the rescalings  $x = \tilde{x}/m$  and  $\phi = 2\tilde{\phi}m^2/\gamma$  in order to put  $S_0$  in the simplified form

$$S_0 = \frac{4m^3}{\gamma^2} \cdot \int d^3\tilde{x} \left[ \frac{(\partial\tilde{\phi})^2}{2} - \frac{\tilde{\phi}^2}{2} - \frac{\tilde{\phi}^3}{3} - \frac{h}{18}\tilde{\phi}^4 \right] = \frac{1}{\lambda} \cdot \tilde{S}. \quad (6)$$

We can now use  $h$  and  $\lambda$  as parameters instead of  $m, \gamma, g$ . The dimensionless parameter  $h \equiv 9gm^2/\gamma^2$ , ranging between 0 and 1, controls the shape of the potential: The barrier is small for small  $h$ , while  $h = 1$  corresponds to two degenerate minima. Method  $\mathcal{B}$  is valid near the thin-wall limit, i.e. for  $h$  close to 1. The dimensionless parameter  $\lambda \equiv \gamma^2/4m^3 = 9g/4mh$  controls the strength of the self-interactions of the field, and, therefore, the size of the loop corrections. This can be seen by rewriting eq. (5) as

$$\tilde{V}_k = \tilde{V}_0 - \frac{\lambda}{12\pi}(\tilde{k}^2 + \tilde{V}_0'')^{3/2} \quad (7)$$

where  $\tilde{k} = k/m$  is a rescaled version of the coarse-graining scale  $k$ .

Before performing the comparison we identify the range of parameters  $h, g$  where both approaches give reliable results. The saddle-point expansion, like any perturbative method, breaks down if the dimensionless coupling  $\lambda$  is too large. In the approach  $\mathcal{A}$  this is signalled by a strong residual dependence of the nucleation rate on the arbitrary coarse-graining scale  $k$  at which the calculation is performed. The origin of the problem

lies in the omission of the important higher-order corrections in the expansion. In the thin-wall limit, for fixed  $\lambda$ , the relative importance of the pre-exponential factor (that we can quantify as  $|\ln A/\ln I|$ , with  $A$  and  $I$  in units of  $m$ ) is minimal and approximately amounts to a  $\lambda \cdot 20\%$  correction. As a result, the saddle-point expansion is meaningful for  $\lambda \lesssim 2$ . The approximation for the saddle-point action employed in method  $\mathcal{B}$  is valid only for  $h$  close to 1. As a result, the comparison of the two methods can be performed only above a certain value of  $h$ . This minimal value of  $h$  increases (decreases) for decreasing (increasing) values of  $\lambda$ . The reason is that the pre-exponential factor in the nucleation rate becomes less (more) important with decreasing (increasing)  $\lambda$ , so that one needs to start from a more (less) accurate approximation for the bubble action in order to have a meaningful comparison. For example one needs  $h \gtrsim 0.8$  when  $\lambda = 1$ . On the other hand, for very large bubbles (in practice when  $h > 0.95$  i.e. when  $\tilde{S} \gtrsim 10^4$ ) it becomes too difficult to determine numerically the saddle point action and the pre-exponential factor, so that method  $\mathcal{A}$  cannot be applied reliably. In conclusion, there is a range of values of  $h$  ( $0.8 < h < 0.95$  for  $\lambda = 1$ ) and of  $\lambda$  ( $\lambda \lesssim 2$ ) where both techniques can be applied and a comparison is possible.

In fig. 1 we display the bubble action (bands) and nucleation rate (lines) in the two approaches as a function of  $h$  for  $\lambda = 1$ . The lower band depicts the value of the bubble action computed from the bare potential in the approach  $\mathcal{B}$ . The band is delimited by  $S_0$ , its exact numerical value (lower thin line), and by  $S_{\mathcal{B}}$ , the analytical approximation for it (upper thick line). The thickness of the band indicates the accuracy of the analytical approximation. The dotted line corresponds to the prediction of method  $\mathcal{B}$  for the nucleation rate  $\ln I$ , with  $I$  in units of  $m$ . The upper band depicts the values of the bubble action  $S_{\mathcal{A}k}$  computed from the coarse-grained potential  $V_k$  for  $m^2 \leq k^2 \leq 2m^2$ . The  $k$ -dependence of  $S_{\mathcal{A}k}$  is compensated by that of the prefactor  $A_{\mathcal{A}k}$ . As a result, the prediction of method  $\mathcal{A}$  for  $\ln I$ , denoted by a continuous line, is  $k$ -independent. The overlap of the dotted and continuous lines indicates that the predictions of the two methods for the bubble-nucleation rate agree when one is not too far from the thin-wall limit.

The region of validity of both approaches leads to large bubble actions, which makes an accurate comparison difficult in fig. 1. For this reason we plot in fig. 2 some useful ratios:

- (a)  $(\ln I_{\mathcal{A}})/S_{\mathcal{A}k}$  for  $m^2 \leq k^2 \leq 2m^2$  (thick band at the bottom);
- (b)  $(\ln I_{\mathcal{B}})/S_{\mathcal{B}}$  (continuous line at the top);
- (c)  $S_0/S_{\mathcal{B}}$  (dashed line);
- (d)  $(\ln I_{\mathcal{A}})/(\ln I_{\mathcal{B}})$  for  $m^2 \leq k^2 \leq 2m^2$  (thin dark band in the middle),
- (e)  $(\ln I_{\mathcal{A}}^{\text{approx}})/(\ln I_{\mathcal{B}})$  for  $m^2 \leq k^2 \leq 2m^2$  (thick light band in the middle), where  $I_{\mathcal{A}}^{\text{approx}}$  is obtained using the following approximation for the prefactor [13, 12]

$$\ln A_{\mathcal{A}k}^{\text{approx}} \approx \frac{\pi k}{2} \left[ - \int_0^\infty r^3 [V_k''(\phi_b(r)) - V_k''(0)] dr \right]^{1/2}. \quad (8)$$

From the form of these ratios the following conclusions can be reached:

- Band (a) shows that the prefactor gives a significant contribution to the total nucleation rate  $\ln I_{\mathcal{A}}$  in approach  $\mathcal{A}$ . The strong  $k$  dependence of this ratio is due to  $S_{\mathcal{A}k}$ . The rate is  $k$ -independent to a very good approximation for  $\lambda \lesssim 1$ .
- Line (b) demonstrates that the prefactor is important also in approach  $\mathcal{B}$ .

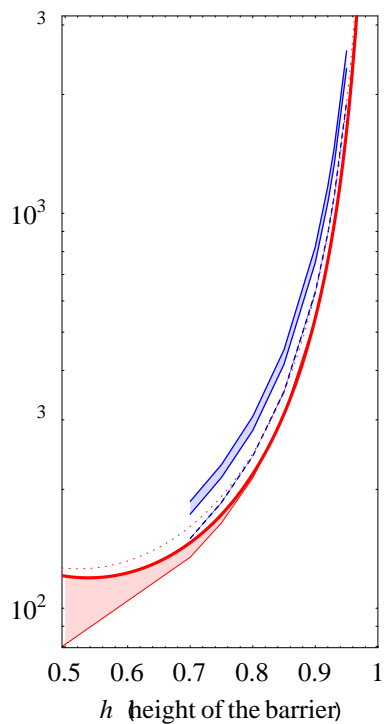


Figure 1: Values of the bubble action and the nucleation rate in the two approaches. See the text for a description.

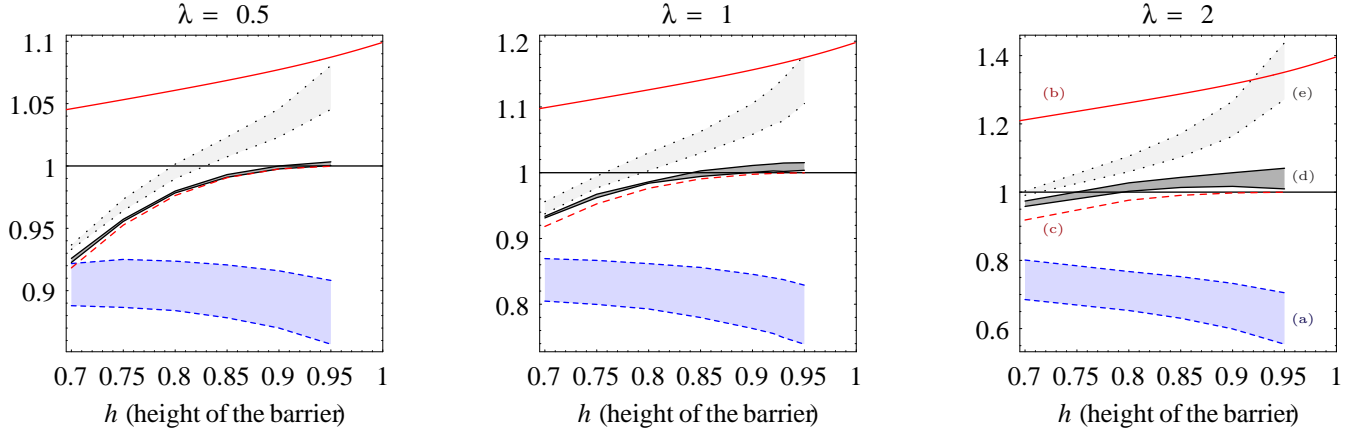


Figure 2: Comparison of the two methods for three different values of the coupling  $\lambda$ . The continuous line (b) at the top of each plot indicates the importance of the prefactor in the approach  $\mathcal{B}$ , estimated through  $(\ln I_{\mathcal{B}})/S_{\mathcal{B}}$ . The thick band at the bottom (a) indicates the importance of the prefactor in the approach  $\mathcal{A}$ , estimated as  $(\ln I_{\mathcal{A}})/S_{\mathcal{A}k}$  and computed for  $m^2 \leq k^2 \leq 2m^2$ . The thin dark band in the middle (d) depicts the ratio of the nucleation rates  $(\ln I_{\mathcal{A}})/(\ln I_{\mathcal{B}})$  computed in the two approaches. The light band (e) depicts  $(\ln I_{\mathcal{A}}^{\text{approx}})/(\ln I_{\mathcal{B}})$ , where  $\ln I_{\mathcal{A}}^{\text{approx}}$  is obtained using the approximation in eq. (8). The dashed line (c) corresponds to  $S_0/S_{\mathcal{B}}$  and indicates how much the approximations of method  $\mathcal{B}$  overestimate the true saddle-point action. All dimensional quantities are in units of  $m$ .

- Line (c) indicates the region of validity of the expansion around the thin-wall approximation employed in approach  $\mathcal{B}$ . The analytical expression for the bubble action  $S_{\mathcal{B}}$  gives a good approximation to the numerically computed  $S_0$  only above a certain value of  $h$  that increases with decreasing  $\lambda$ .
- The small width of band (d) indicates that the  $k$  dependence of  $\ln I_{\mathcal{A}}$  is very weak. This verifies that approach  $\mathcal{A}$  is reliable. The fact that band (d) is close to one, demonstrates that the two approaches agree very well when they are both reliable.
- Away from the thin-wall limit,  $S_{\mathcal{B}}$  overestimates the true bubble action  $S_0$ . At  $h \approx 0.7$ , for example,  $S_{\mathcal{B}}$  is  $\sim 10\%$  larger than  $S_0$ . For  $\lambda \lesssim 1$  the approximated prefactor is small,  $|\ln A_{\mathcal{B}}| \lesssim 10\% \cdot S_{\mathcal{B}}$ , and presumably has a only a  $\sim 10\%$  error. As a result, method  $\mathcal{B}$  is not sufficiently accurate and the two approaches do not agree. However, the fact that line (c) and band (d) deviate from 1 in exactly the same way indicates that the disagreement is largely caused by the inaccurate determination of  $S_0$ , while the estimates of the prefactors in the two approaches are in agreement.
- Bands (d) and (e) are in good agreement below the value of  $h$  at which the approach  $\mathcal{B}$  stops being reliable. This makes it possible to extend the region of  $h$  for which an analytical expression for the nucleation rate is available. Near the thin wall limit ( $h$  close to 1), the analytical expression provided by method  $\mathcal{B}$  (eq. (138) or eq. (147) of ref. [16]) can be used. For smaller  $h$ , when the expansion around the thin-wall approximation breaks down (as can be checked by comparing eq. (54) of ref. [16] with a numerical determination of the bubble action) eq. (8) can be used.

Finally, we point out that in approach  $\mathcal{A}$  fluctuations around the bubble (taken into account by the prefactor) enhance the nucleation rate with respect to  $\exp(-S_{\mathcal{A}k})$ . On the other hand, in approach  $\mathcal{B}$  the nucleation rate is smaller than its tree-level approximation, when the comparison is performed at fixed values of the bare parameters. This does not indicate a discrepancy. The prefactor enhances the nucleation rate in approach  $\mathcal{B}$  as well, if the comparison is done at fixed values of the physical mass and couplings defined at the true minimum [16].

## 4 Conclusions

In their joint region of validity the two methods for the calculation of the nucleation rate, based on coarse-grained potentials on the one hand and on dimensional regularization on the other, agree very well, thus giving support to their reliability.

**Acknowledgments** The work of N.T. was supported by the E.C. under TMR contract No. ERBFMRX-CT96-0090 and contract No. ERBFMBICT983132.

## References

- [1] F.F. Abraham, *Homogeneous Nucleation Theory*, (Academic Press, New York, 1974).
- [2] *Dynamics of First-Order Phase Transitions*, eds. H.J. Herrmann, W. Janke and F. Karsch (World Scientific, Singapore, 1992).
- [3] J.D. Gunton, M. San Miguel and P.S. Sahni, in *Phase Transitions and Critical Phenomena*, Vol. 8, eds. C. Domb and J.L. Lebowitz (Academic Press, London, 1983).
- [4] K. Binder, Rep. Prog. Phys. **50**, 783 (1987).
- [5] P.A. Rikvold and B.M. Gorman, Ann. Rev. Comput. Phys. I, ed. D. Stauffer, p. 149 (World Scientific, Singapore, 1994).
- [6] J. Langer, Ann. Phys. **41**, 108 (1967); *ibid.* **54**, 258 (1969); Physica **73**, 61 (1974).
- [7] W.N. Cottingham, D. Kalafatis and R. Vinh Mau, Phys. Rev. B **48**, 6788 (1993); J. Baacke and V.G. Kiselev, Phys. Rev. D **48**, 5648 (1993); J. Baacke, *ibid.* **52**, 6760 (1995); J. Kripfganz, A. Laser and M.G. Schmidt, Nucl. Phys. B **433**, 467 (1995); M. Gleiser, G.C. Marques and R.O. Ramos, Phys. Rev. D **48**, 1571 (1993); G.H. Flores, R.O. Ramos and N.F. Svaiter, Int. J. Mod. Phys. A **14**, 3715 (1999); D.G. Barci, E.S. Fraga and C.A.A. de Carvalho, Phys. Rev. D **55**, 4947 (1997).
- [8] P.A. Rikvold, Prog. Theor. Phys. Suppl. **99**, 95 (1989); Physica Scripta **T38**, 36 (1991).
- [9] S. Coleman, Phys. Rev. D **15**, 2929 (1977); C.G. Callan and S. Coleman, Phys. Rev. D **16**, 1762 (1977).
- [10] I. Affleck, Phys. Rev. Lett. **46**, 388 (1981); A.D. Linde, Nucl. Phys. B **216**, 421 (1983).
- [11] N. Tetradis and C. Wetterich, Nucl. Phys. B **398**, 659 (1993); Int. J. Mod. Phys. A **9**, 4029 (1994).
- [12] A. Strumia, N. Tetradis and C. Wetterich, Phys. Lett. B **467**, 279 (1999).
- [13] A. Strumia and N. Tetradis, Nucl. Phys. B **542**, 719 (1999) and JHEP **9911**, 023 (1999).
- [14] K.G. Wilson, Phys. Rev. B **4**, 3174 and 3184 (1971); K.G. Wilson and J. Kogut, Phys. Rep. **12**, 75 (1974); F.J. Wegner, in: *Phase Transitions and Critical Phenomena*, vol. 6, eds. C. Domb and M.S. Green (Academic Press, New York, 1976).
- [15] C. Wetterich, Nucl. Phys. B **352**, 529 (1991); Z. Phys. C **57**, 451 (1993); *ibid.* **60**, 461 (1993); C. Wetterich, Phys. Lett. B **301**, 90 (1993); N. Tetradis and C. Wetterich, Nucl. Phys. B **422**, 541 (1994).
- [16] G. Münster and S. Rotsch, Eur. Phys. J. C **12**, 161 (2000).
- [17] G. Münster and J. Heitger, Nucl. Phys. B **424**, 582 (1994).